Published in final edited form as:

Laryngoscope. 2016 December ; 126(12): E387–E395. doi:10.1002/lary.26215.

Antiangiogenic Antibody Improves Melanoma Detection by Fluorescently Labeled Therapeutic Antibodies

Larissa Sweeny, MD[1], **Andrew Prince, BS**[2], **Neel Patel, MD**[3], **Lindsay S. Moore, MD**[1], **Eben L. Rosenthal, MD**[4], **Brian B. Hughley, MD**[1], and **Jason M. Warram, PhD**[1,*]

[1]Department of Otolaryngology – Head and Neck Surgery, University of Alabama at Birmingham, Birmingham, Alabama

[2]University of Alabama School of Medicine at Birmingham, Birmingham, Alabama

[3]Department of Psychiatry, University of Alabama at Birmingham, Birmingham, Alabama

[4]Department of Otolaryngology, Stanford University, Stanford, California

Abstract

Objective—Evaluate if vascular normalization with an antiangiogenic monoclonal antibody improves detection of melanoma using fluorescently labeled antibody-based imaging.

Study Design—Preclinical.

Methods—Panitumumab and control IgG were covalently linked to a near-infrared fluorescent probe (IRDye800CW). Immunodeficient mice with ear xenografts of melanoma cell lines (A375 and SKMEL5) were systemically injected (200μg, tail vein) with either IgG-IRDye800CW, panitumumab-IRDye800CW, or combination (bevacizumab (5mg/kg) administered 72 hours pre panitumumab-IRDye800CW)(n=5). Primary tumors were imaged with open-field (LUNA) and closed-field (Pearl) imaging devices. Postresection, the concentration of labeled antibody within the tumor (μg/g) was calculated using normalized standards.

Results—The mean fluorescence within the melanoma tumors was greater for the combination group compared to panitumumab alone for both cell lines ($p<0.001$). The tumor-to-background ratio (TBR) for the A375 tumors was greater for the combination (3.4–7.1) compared to the panitumumab alone (3.2–5.0)($p=0.04$). The TBR for SKMEL5 tumors was greater for the combination (2.4–6.0) compared to the panitumumab alone (2.2–3.9)($p=0.02$). Within A375 tumors, the concentration was lower for panitumumab (0.51μg/g) compared to combination group (0.68μg/g)($p=0.036$). Within SKMEL5 tumors, the concentration was lower for panitumumab (0.0.17μg/g) compared to combination group (0.35μg/g)($p=0.048$). Residual tumor (1.0–0.2 mg) could be differentiated from background in both panitumumab and combination groups. For both cell lines, panitumumab and combination groups had greater mean fluorescence of the tumor compared to control IgG.

[*]**Corresponding Author:** Jason Warram PhD, MD, UAB – Department of Otolaryngology, Volker Hall G082, 1670 University Blvd, Birmingham, AL 35233, Tel: (205) 934-9766, Fax: (205) 934-3993, mojack@uab.edu.

Financial disclosure of authors and reviewers: None reported.

Conflicts of Interest: None

Conclusions—The addition of antiangiogenic therapy improves uptake of fluorescently labeled monoclonal antibodies within melanoma tumors. Clinical translation could improve detection of melanoma intraoperatively, reducing positive margins and sparing normal tissue.

Keywords

Cutaneous; head and neck; melanoma; optical imaging; antibody; fluorescence

INTRODUCTION

Cutaneous malignancies comprise more than two-thirds of newly diagnosed cancers in the United States, with greater than one million cases diagnosed each year.[1] While melanoma makes up only 3% of all skin cancers, it accounts for 83% of skin cancer deaths.[2] Despite the onset of novel therapeutics, melanoma incidence and mortality rates have been on the rise.[3–5] Inadequate surgical margins can lead to the development of local recurrence and distant metastasis, which is associated with a dismal prognosis. Approximately 40–60% of patients who develop recurrent melanoma die from their disease.[6,7]

We have shown previously that fluorescently labeled monoclonal antibody, panitumumab (Vectabix), can detect melanoma using near infrared (NIR) imaging.[8] Panitumumab binds to the extracellular domain of epidermal growth factor receptor (EGFR). EGFR is a transmembrane tyrosine kinase involved in the regulation of cell differentiation and proliferation.[9–11] The role of EGFR in tumor progression and the correlation between EGFR overexpression and survival of patients with squamous cell carcinomas has been extensively studied.[10,12–19] However, EGFR expression by melanoma cells is less understood. Previous studies found EGFR expression levels in melanoma correlated with prognosis.[20–25] While melanocytes do not express EGFR,[23–25] there is an increase in EGFR expression as melanocytic lesions undergo progression from dysplasia, to primary melanoma and ultimately to metastatic melanoma.[26] Clinically, EGFR expression has been found to correlate with sentinel lymph nodes in patients with melanoma.[27] Furthermore, in metastatic melanoma there is increased activity of signaling pathways downstream of EGFR.[28]

Melanoma cells also secrete high levels of vascular endothelial growth factor (VEGF).[29–31] Previous publications found that VEGF is critical to the angiogenesis of a tumor.[32–34] This led to the development and clinical use of bevacizumab (Avastin), a monoclonal antibody targeting VEGF.[29–31] Compared to normal vasculature, tumor vasculature is circuitous with sporadic pericyte coverage, endothelial gaps, and variations in basement membrane thickness.[32,35,36] Subsequently, the vascular permeability and interstitial pressure increase.[32,35,36] Targeting VEGF induces vessel normalization, which is characterized by a reduction in the number and diameter of immature vessels, increased pericyte coverage and decreased interstitial pressure.[32,35,36] This reduces drug egress and improves drug delivery. Bevacizumab in combination with other anticancer therapies has been shown to improve therapeutic efficacy of these agents in other malignancies.[37–40] Therefore we hypothesize that pretreatment with bevacizumab will increase the uptake of fluorescently labeled panitumumab in the melanoma tumors and improve tumor-to-background ratio (TBR).

MATERIALS AND METHODS

Cell Lines and Cell Culture

Melanoma cell lines A375 and SKMEL5 (ATCC, Manassas, VA) were maintained in Dulbecco's modified Eagle's medium containing 10% fetal bovine serum and supplemented with 1% penicillin, streptomycin and amphotericin B and were incubated at 37°C in 5% CO2.

Animal Models

Nude and severe combined immunodeficient female mice, aged 4–6 weeks (Charles River Laboratories, Hartford, Connecticut), were obtained, housed, experiments conducted and animal euthanasia performed in accordance with the University of Alabama at Birmingham Institutional Animal Care and Use Committee guidelines (Animal Protocol Number: IACUC-09904). All institutional and national guidelines for the care and use of laboratory animals were followed. The mice received injections of 2×10^6 A375 or SKMEL5 cells suspended in 200 μL of phosphate buffered solution into the dorsum of the ear. Each cohort included 5 mice.

Fluorescence Labeling of Monoclonal Antibodies

IRDye800CW (IRDye800CW-N-hydroxysuccinimide ester, LI-COR Biosciences, Lincoln, Nebraska) is nontoxic to mice.[41] IRDye800CW is a near infrared imaging probe with a broad absorption (778 nm) and emission (794 nm) peaks. Antibody conjugation results in an absorption of 774 nm and an emission of 789 nm.[42,43] Control IgG (Innovative Research, Peary Court Novi, MI) and panitumumab (Vectibix; Amgen, Thousands Oaks, California) were labeled according to the manufacturer's instructions. Briefly, antibodies were incubated with IRDye800CW in 1.00 M potassium phosphate buffer (pH 9.0) for 2 hrs at room temperature. Desalting spin columns (Pierce Biotechnology, Rockford, IL) removed the unconjugated dye. A final dye:protein ratio of 1.5–2.0 was determined using spectrophotometry.

Western Blot Analysis of EGFR and VEGF Expression by Melanoma Cell In Vitro

Cells were grown to 70%–80% confluence, washed twice with cold PBS, and lysed [lysis buffer: 50mM Tris-HCl (pH7.5), 150mM NaCl, 1% (v/v) NP40, 0.5% (w/v) sodium deoxycholate, 1mM EDTA, 0.1% SDS and a protease inhibitor cocktail (Roche Applied Science, Indianapolis, IN)]. Lysates were collected by centrifugation at 12000 × g for 20 mins at 40°C. BCA protein assay (Thermo Scientific, Rockford, IL) measured protein concentrations. Lysates with 10 μg of total protein were resolved by SDS PAGE and transferred to PVDF membranes. Membranes were incubated with the primary antibody (EGFR, Abcam, #15669 and VEGF, Abcam, #46154), washed, incubated with horseradish peroxidase conjugated secondary antibodies, washed again and detected by the Amersham ECL Western blotting detection system (GE healthcare, Buckinghamshire, UK). Membranes were reprobed with horseradish peroxidase-conjugated mouse monoclonal antihuman beta-actin.

Histologic Analysis of Melanoma Tumors Grown In Vivo

Standard hematoxylin and eosin (H&E) staining was done for all tumor specimens (Figure 1). Human melanoma black (HMB-45) staining was chosen for its high specificity for melanoma. Immunohistochemical (IHC) analysis was performed to determine EGFR and Ki67 expression levels. Ki67 allowed for comparison of the cell viability between the groups.

Samples were rehydrated in xylene, 95% ethanol, and 70% ethanol. Antigen retrieval was in 1 mM EDTA, pH 9.0, for 5 minutes at 100°C. Samples were cooled at room temperature and blocked with 5% BSA in TBST for 5 minutes. Primary antibody, EGFR (Abcam, #27600), HMB-45 (Abcam, #787) or Ki67 antibody (Abcam, #15580), was applied at the concentrations recommended and incubated for 1 hour. Secondary antibody (Pierce goat anti-rabbit HRP, #32260) was applied for 40 minutes in a humidified chamber at room temperature. DAB substrate was applied to slides and allowed to incubate at room temperature until appropriate color developed. Samples were counterstained with Harris Hematoxylin diluted 1:1 with tap water for 45 seconds. Finally, samples were dehydrated, counted with Permount and allowed to dry overnight.

Described previously, semiquantitative analysis of EGFR was performed for both staining intensity and quality by two independent observers blinded to the cohorts and each other (LS and AP). Scoring values were assigned as follows: 0=none to <10% of tumor cells staining, 1+=light and incomplete staining in >10% of tumor cells, 2+=moderate and complete staining of >10% of tumor cells and 3+=intense and complete staining >10%.[44,45] For the Ki67 scoring index, five sections of melanoma cells were selected. The melanoma cells were counted for the section and the percentage positive for Ki67 was recorded.

In Vivo NIR Imaging of Melanoma Tumors

Once tumor growth reached an average size of 8 × 8 mm, the mice were systemically injected (200μg, tail vein) with IgG-IRDye800CW or panitumumab-IRDye800CW (n=5). The combination group received systemic injection of bevacizumab (5mg/kg, tail vein) three days prior to panitumumab-IRDye800CW (n=5). Previous studies found 3 days to be optimal for vessel normalization by bevacizumab.[46] Primary tumors were imaged daily and harvested on day 14. The tumors were serially sectioned, reducing the tumor volume in half with each resection. Tumor specimens 4mm thick were imaged and weighed. True positives based on imaging were histologically confirmed.

Quantification of Fluorescently Labeled Antibody within Melanoma Tumors

The concentration of labeled antibody per gram of tumor (μg/g) was calculated using normalized standards with known concentrations of panitumumab-IRDye800CW or IgG-IRDye800CW (Supplemental Figure 1B).[46] Known concentrations of labeled antibody (0.0125–1.61 μg) were quantified by drawing a region of interest around the internal rim of the well and recording the mean pixel values. A linear standard of total fluorescence counts-

Supplemental Figure 1: (A) Western blot analysis for quantification of protein expression levels of epidermal growth factor receptor (EGFR) and vascular endothelial growth factor (VEGF). (B) Example of normalized standards used for calculation of fluorescently labeled antibody concentration within the melanoma tumors.

to-microgram of dye was calculated. The tumor mean pixel fluorescence value acquired from a 4mm thick section of tumor was compared to the standard yielding a microgram of dye value. This was divided by the tumor weight (grams) and injected dose of IRDye800CW (200 μg) to yield a percent injected dose per gram (%ID/g).[46]

NIR Imaging Devices Used for In Vivo Imaging

The Pearl Impulse (LI-COR Biosciences, Lincoln, Nebraska) is a closed system with a cooled charge-coupled camera. The TBR was derived by dividing the mean fluorescence of the tumor by the mean fluorescence of the background (mouse flank).[43]

The LUNA (Novadaq, Toronto, Ontario, Canada) is an open-field imaging device using a charged coupled video camera to capture fluorescence (30 frames/second).[8,47] LUNA was used for real-time fluorescent-guided resection of the tumors.

Statistical Analyses

There were 5 measurements for each group at each time point. Mean and standard deviation were calculated and plotted for continuous variables. Bar graphs represent mean values and error bars represent standard deviation. Statistical significance between groups was determined by a t-test (two sided) or if data did not normally distribute a Wilcoxon test. Statistical analysis was performed by the lead author and principal investigator. A $p<0.05$ was considered statistically significant. Western blot band intensities were quantified in triplicate using ImageJ (http://rsb.info.nih.gov/ij/) and normalized to beta-actin.

RESULTS

EGFR and VEGF Expression by Melanoma Cells

Western blot analysis was used determine EGFR and VEGF expression by the two melanoma cell lines in vitro. On western blot analysis, A375 cells were found to have a two-fold greater EGFR expression level compared to SKMEL5 cells ($p<0.001$). Additionally, A375 cells were found to have six-fold greater VEGF expression compared to SKMEL5 cells ($p<0.0001$)(Supplemental Figure 1A).

IHC analysis was used to determine EGFR expression by the melanoma tumors (A375 and SKMEL5) in vivo. On IHC analysis, EGFR expression levels were found to be low to moderate for both cell lines, consistent with findings of previous publications (Figure 1).[48,49] The mean EGFR score for A375 was 1.5 (±0.5) and for SKMEL5 was 1.3 (±0.45) ($p=0.63$). Interestingly, there was greater EGFR membrane staining for the A375 tumors compared SKMEL5 tumors, which had predominately a cytoplasmic EGFR staining pattern. For the A375 tumors, the mean EGFR expression for the panitumumab only group was 1.7 (±0.58) compared to 1.4 (±0.55) for the combination therapy group ($p=0.54$). For the SKMEL5 tumors, the mean EGFR expression for the panitumumab only group was 1.2 (±0.41) compared to 1.3 (±0.52) for the combination therapy group ($p=0.84$).

Ki67 staining of the tumors was used to determine viability and ensure one time treatment with either panitumumab or combination therapy did not result in significant cancer cell death. Using the Ki67 scoring index, there was no statistical difference between treatment

groups or cell lines (Figure 1). For the A375 tumors, the mean in the panitumumab only group was 68% (±12%) compared to 54% (±8%) in the combination therapy group (p=0.10). For the SKMEL5 tumors, the mean in the panitumumab only group was 48% (±7%) compared to 43% (±8%) in the combination therapy group (p=0.32).

NIR Fluorescent Imaging of Melanoma Tumors In Vivo

Daily imaging with the Pearl was done following systemic injection of either panitumumab-IRDye800CW or IgG-IRDye800CW (Figure 2). There was a greater mean fluorescence within the A375 melanoma tumors compared to background for the panitumumab (range 0.3–0.93) and the combination (range 0.22–0.84) groups at each imaging time point ($p<0.001$; Figure 3). Likewise, there was a greater mean fluorescence within the SKMEL5 melanoma tumors compared to background for the panitumumab (days 3–14, range 0.14–0.52) and the combination (days 1–14, range 0.17–0.76) groups ($p<0.001$; Figure 3). While the combination therapy resulted in equivocal mean fluorescence in the SKMEL5 tumors compared to the A735 tumors (p=0.17), the panitumumab alone resulted in a lower mean fluorescence in the SKMEL5 tumors compared to the A375 tumors (p=0.03). Consistent with previous publications, panitumumab-IRDye800CW resulted in a greater mean fluorescence within the melanoma tumors at all time points compared to control IgG-IRDye800CW for both cell lines.[8,50–52]

Antiangiogenic Therapy Improves Contrast-Enhanced Tumor Delineation

To determine the ability of fluorescence imaging (using the Pearl Impulse) to differentiate tumor from normal tissue, TBR were calculated. For the A375 tumors, combination therapy (range 3.4–7.1) had statistically greater TBR than the panitumumab alone (range 3.2–5.0) (p=0.04; Figure 4). For the SKMEL5 tumors, combination therapy (range 2.4–6.0) also had significantly greater TBR than the panitumumab alone (range 2.2–3.9)(p=0.02; Figure 4). For both cell lines, the use of combination therapy resulted in greater TBR compared to the control IgG treated group ($p<0.05$).

Residual Tumor Detection in Melanoma Tumors In Vivo

Fluorescence guided surgical resection was done with the LUNA at the time of tumor harvest. For the A375 tumors, the lowest tumor mass which could be differentiated from the background wound bed fluorescence was 1.5 mg for panitumumab alone and 0.20 mg for the combination group (Figure 5). For the SKMEL5 tumors, the lowest tumor mass which could be differentiated from the background wound bed fluorescence for panitumumab alone was 0.60 mg and for the combination group was 1.0 mg (Figure 5).

Quantification of Fluorescently Labeled Antibody within Melanoma Tumors

The concentrations of labeled antibody within the A375 tumors was greater for the combination group (0.68 μg/g; 0.34 %ID/g) compared to panitumumab alone (0.51 μg/g; 0.25 %ID/g)(p=0.038) and IgG (0.02 μg/g; 0.01 %ID/g) groups (p=0.001; Figure 6). Similarly, the concentrations of labeled antibody within the SKMEL5 tumors was greater for the combination group (0.35 μg/g; 0.17 %ID/g) compared to panitumumab alone (0.17 μg/g; 0.08 %ID/g) and IgG (0.16 μg/g; 0.08 %ID/g) groups ($p<0.05$; Figure 6).

DISCUSSION

Surgical resection of melanoma remains a challenge as the disease is often non-palpable, margins are determined based on tumor thickness, and frozen section analysis is unreliable. As a result, there is a need for improvements in melanoma detection, to improve survival and reduce the morbidity associated with resection. Currently there is no cancer specific contrast agent available for use in the clinic or the operating room for melanoma. Development of an imaging agent that can be used in real-time to detect melanoma cells has the potential to reduce positive margins and improve outcomes.

During in vivo imaging, the A375 tumors had greater mean fluorescence and concentration of panitumumab-IRDye800CW compared to SKMEL5 tumors. This is due to variations in the expression levels and cellular location of EGFR between the cell lines. In vitro, the A375 cells had 2-fold greater EGFR expression levels compared to SKMEL5 cells. In vivo, EGFR is predominately on the cell surface of A375 tumors cells compared to intracytoplasmic for the SKMEL5 tumor cells. Therefore, the higher fluorescence in the A375 tumors is likely due to greater availability (expression levels and membrane location) of the EGFR for panitumumab-IRDye800CW binding.

The effect of antiangiogenic therapy on the uptake of fluorescently labeled antibodies within melanoma tumors was evaluated by pretreating with bevacizumab. When comparing the mean fluorescence of the A375 melanoma tumors, the combination therapy group had a similar mean fluorescence to that of the panitumumab-IRDye800CW only treatment group. However, in the SKMEL5 tumors, there was a greater mean fluorescence within the melanoma tumors of the combination therapy group compared to the panitumumab-IRDye800CW alone group. These findings suggest that through vessel normalization and prevention of drug egress, pretreatment with bevacizumab results in improved delivery of pantintumab-IRDye800CW into melanoma tumors with lower EGFR expression.[53–55]

Similar to findings in previous publications, proliferation of SKMEL5 in vitro and in vivo was lower compared to A375.[56] Since the SKMEL cells are proliferating at a slower rate, we anticipated they would secrete lower concentrations of growth factors. This was confirmed with western blot analysis, which found A375 to have a 6-fold greater VEGF expression compared SKMEL5 cells. With less VEGF available, administration of the same dose of bevacizumab will have a greater impact on downstream pathways, including vessel normalization, in SKMEL5 tumors compared to A375 tumors. Previously, SKMEL5 cells were found to be more sensitive to survivin inhibition. While another investigation found SKMEL5 cells were more sensitive than A375 cells to treatment with sorafenib, a VEGF and Braf inhibitor with antiangiogenic and kinase inhibition properties.[57] While these agents target different pathways, they support the findings in our study that SKMEL5 cells are more sensitive to the effects of therapy. Additionally, both bevacizumab and sorafenib inhibit VEGF and subsequently induce vessel normalization.[32,56,58] These differences in A375 and SKMEL5 behavior are multifactorial and likely due to variations in proliferation rates, microvessel density, behavior of tumor endothelial and pericyte cells, and EGFR turnover/internalization rates.

We also investigated the ability of fluorescence imaging to delineate tumor from normal tissue by calculating TBR. In vivo, we found pretreatment with bevacizumab resulted in greater TBR for the combination therapy groups compared to panitumumab-IRDye800CW only treatment groups in both cell lines. These findings demonstrate that pretreatment with bevacizumab improves tumor specific uptake of panitumumab-IRDye800CW relative to normal tissue. The ability to differentiate tumor from normal tissue is important for improving detection of residual disease, reducing positive margin rates, and preserving normal, uninvolved tissues.

Clinical translation has the potential to improve early detection rates and surgical resection of melanoma. The near infrared spectral range of IRDye800CW (700–900 nm) decreases artifact of autofluorescence and improves depth of penetration.[8,59,60] The use of agents already approved by the FDA (panitumumab) and equipment currently available in the operating room (LUNA) allows for a faster transition from preclinical to clinical and for more cost-effective implementation.

CONCLUSION

Molecularly targeted antibodies for cancer treatment are rapidly evolving. With the increased interest in fluorescent optical imaging probes and devices, the potential for significant improvements in intraoperative surgical techniques and identification of residual disease exist. Identifying which agents and combination therapy provides the greatest TBR, and subsequently greatest specificity and sensitivity, is important in the translatability of these agents. In vivo, pretreatment with bevacizumab prior to administration of panitumumab-IRDye800CW improved the TBR compared to panitumumab-IRDye800CW alone. In addition to its improved tumor localization, it is FDA approved, making it an optimal antibody for clinical translation.[43] To our knowledge, this is the first study to investigate the effects of bevacizumab on the uptake of monoclonal antibodies targeting EGFR in melanoma tumors. With the rising incidence of melanoma and high mortality, novel methods of detection are paramount to improving outcomes.

Acknowledgments

The authors would like to thank Yolanda Hartman for performing the histochemical staining and western blot. Equipment was donated by Novadaq and LICOR Biosciences. This work was supported by grants from the National Institute of Health (R21CA179171 and T32 CA091078).

REFRENCES

1. Dhawan AP, D'Alessandro B, Patwardhan S, Mullani N. Multispectral optical imaging of skin-lesions for detection of malignant melanomas. Conf Proc IEEE Eng Med Biol Soc. 2009; 2009:5352–5355. [PubMed: 19964673]
2. Tannous Z, Al-Arashi M, Shah S, Yaroslavsky AN. Delineating melanoma using multimodal polarized light imaging. Lasers Surg Med. 2009; 41:10–16. [PubMed: 19143015]
3. Simard EP, Ward EM, Siegel R, Jemal A. Cancers with increasing incidence trends in the United States: 1999 through 2008. CA Cancer J Clin. 2012
4. Leachman SA, Cassidy PB, Chen SC, et al. Methods of Melanoma Detection. Cancer treatment and research. 2016; 167:51–105. [PubMed: 26601859]

5. Siegel R, Ma J, Zou Z, Jemal A. Cancer statistics, 2014. CA Cancer J Clin. 2014; 64:9–29. [PubMed: 24399786]
6. Nguyen QT, Olson ES, Aguilera TA, et al. Surgery with molecular fluorescence imaging using activatable cell-penetrating peptides decreases residual cancer and improves survival. Proc Natl Acad Sci U S A. 2010; 107:4317–4322. [PubMed: 20160097]
7. Riker AI, Glass F, Perez I, Cruse CW, Messina J, Sondak VK. Cutaneous melanoma: methods of biopsy and definitive surgical excision. Dermatol Ther. 2005; 18:387–393. [PubMed: 16297013]
8. Day KE, Beck LN, Deep NL, Kovar J, Zinn KR, Rosenthal EL. Fluorescently labeled therapeutic antibodies for detection of microscopic melanoma. Laryngoscope. 2013; 123:2681–2689. [PubMed: 23616260]
9. Hynes NE, Lane HA. ERBB receptors and cancer: the complexity of targeted inhibitors. Nature reviews Cancer. 2005; 5:341–354. [PubMed: 15864276]
10. Kalyankrishna S, Grandis JR. Epidermal growth factor receptor biology in head and neck cancer. Journal of clinical oncology: official journal of the American Society of Clinical Oncology. 2006; 24:2666–2672. [PubMed: 16763281]
11. Herbst RS. Review of epidermal growth factor receptor biology. International journal of radiation oncology, biology, physics. 2004; 59:21–26.
12. Ang KK, Berkey BA, Tu X, et al. Impact of epidermal growth factor receptor expression on survival and pattern of relapse in patients with advanced head and neck carcinoma. Cancer research. 2002; 62:7350–7356. [PubMed: 12499279]
13. Ch'ng S, Low I, Ng D, et al. Epidermal growth factor receptor: a novel biomarker for aggressive head and neck cutaneous squamous cell carcinoma. Human pathology. 2008; 39:344–349. [PubMed: 18045646]
14. Eriksen JG, Steiniche T, Askaa J, Alsner J, Overgaard J. The prognostic value of epidermal growth factor receptor is related to tumor differentiation and the overall treatment time of radiotherapy in squamous cell carcinomas of the head and neck. International journal of radiation oncology, biology, physics. 2004; 58:561–566.
15. Numico G, Russi EG, Colantonio I, et al. EGFR status and prognosis of patients with locally advanced head and neck cancer treated with chemoradiotherapy. Anticancer research. 2010; 30:671–676. [PubMed: 20332488]
16. Quon H, Liu FF, Cummings BJ. Potential molecular prognostic markers in head and neck squamous cell carcinomas. Head & neck. 2001; 23:147–159. [PubMed: 11303632]
17. Rubin Grandis J, Melhem MF, Gooding WE, et al. Levels of TGF-alpha and EGFR protein in head and neck squamous cell carcinoma and patient survival. Journal of the National Cancer Institute. 1998; 90:824–832. [PubMed: 9625170]
18. Rubin Grandis J, Tweardy DJ, Melhem MF. Asynchronous modulation of transforming growth factor alpha and epidermal growth factor receptor protein expression in progression of premalignant lesions to head and neck squamous cell carcinoma. Clinical cancer research: an official journal of the American Association for Cancer Research. 1998; 4:13–20. [PubMed: 9516947]
19. Temam S, Kawaguchi H, El-Naggar AK, et al. Epidermal growth factor receptor copy number alterations correlate with poor clinical outcome in patients with head and neck squamous cancer. Journal of clinical oncology: official journal of the American Society of Clinical Oncology. 2007; 25:2164–2170. [PubMed: 17538160]
20. Boone B, Jacobs K, Ferdinande L, et al. EGFR in melanoma: clinical significance and potential therapeutic target. J Cutan Pathol. 38:492–502.
21. Boone B, Brochez L. Clinical markers and driving mechanisms in melanoma progression: VEGF-C, RhoC, c-Ski/SnoN and EGFR. Verh K Acad Geneeskd Belg. 2009; 71:251–294. [PubMed: 20232784]
22. Rakosy Z, Vizkeleti L, Ecsedi S, et al. EGFR gene copy number alterations in primary cutaneous malignant melanomas are associated with poor prognosis. Int J Cancer. 2007; 121:1729–1737. [PubMed: 17594688]
23. Grahn JC, Isseroff RR. Human melanocytes do not express EGF receptors. The Journal of investigative dermatology. 2004; 123:244–246. [PubMed: 15191569]

24. Real FX, Rettig WJ, Chesa PG, Melamed MR, Old LJ, Mendelsohn J. Expression of epidermal growth factor receptor in human cultured cells and tissues: relationship to cell lineage and stage of differentiation. Cancer research. 1986; 46:4726–4731. [PubMed: 3015394]
25. Sparrow LE, Heenan PJ. Differential expression of epidermal growth factor receptor in melanocytic tumours demonstrated by immunohistochemistry and mRNA in situ hybridization. The Australasian journal of dermatology. 1999; 40:19–24. [PubMed: 10098284]
26. deWit PE, Moretti S, Koenders PG, et al. Increasing epidermal growth factor receptor expression in human melanocytic tumor progression. The Journal of investigative dermatology. 1992; 99:168–173. [PubMed: 1629628]
27. Boone B, Jacobs K, Ferdinande L, et al. EGFR in melanoma: clinical significance and potential therapeutic target. J Cutan Pathol. 2011; 38:492–502. [PubMed: 21352258]
28. Mirmohammadsadegh A, Mota R, Gustrau A, et al. ERK1/2 is highly phosphorylated in melanoma metastases and protects melanoma cells from cisplatin-mediated apoptosis. The Journal of investigative dermatology. 2007; 127:2207–2215. [PubMed: 17508026]
29. Redondo P, Bandres E, Solano T, Okroujnov I, Garcia-Foncillas J. Vascular endothelial growth factor (VEGF) and melanoma. N-acetylcysteine downregulates VEGF production in vitro. Cytokine. 2000; 12:374–378. [PubMed: 10805219]
30. Gonzalez-Cao M, Viteri S, Diaz-Lagares A, et al. Preliminary results of the combination of bevacizumab and weekly Paclitaxel in advanced melanoma. Oncology. 2008; 74:12–16. [PubMed: 18536525]
31. Terheyden P, Hofmann MA, Weininger M, Brocker EB, Becker JC. Anti-vascular endothelial growth factor antibody bevacizumab in conjunction with chemotherapy in metastasising melanoma. J Cancer Res Clin Oncol. 2007; 133:897–901. [PubMed: 17583821]
32. Arjaans M, Schroder CP, Oosting SF, Dafni U, Kleibeuker JE, de Vries EG. VEGF pathway targeting agents, vessel normalization and tumor drug uptake: from bench to bedside. Oncotarget. 2016
33. Ferrara N, Gerber HP, LeCouter J. The biology of VEGF and its receptors. Nature medicine. 2003; 9:669–676.
34. Kerbel RS. Tumor angiogenesis. The New England journal of medicine. 2008; 358:2039–2049. [PubMed: 18463380]
35. Carmeliet P, Jain RK. Principles and mechanisms of vessel normalization for cancer and other angiogenic diseases. Nature reviews Drug discovery. 2011; 10:417–427. [PubMed: 21629292]
36. Jain RK. Normalizing tumor microenvironment to treat cancer: bench to bedside to biomarkers. Journal of clinical oncology: official journal of the American Society of Clinical Oncology. 2013; 31:2205–2218. [PubMed: 23669226]
37. Blagosklonny MV. Antiangiogenic therapy and tumor progression. Cancer cell. 2004; 5:13–17. [PubMed: 14749122]
38. Blagosklonny MV. How Avastin potentiates chemotherapeutic drugs: action and reaction in antiangiogenic therapy. Cancer biology & therapy. 2005; 4:1307–1310. [PubMed: 16322683]
39. Bottsford-Miller JN, Coleman RL, Sood AK. Resistance and escape from antiangiogenesis therapy: clinical implications and future strategies. Journal of clinical oncology: official journal of the American Society of Clinical Oncology. 2012; 30:4026–4034. [PubMed: 23008289]
40. Jayson GC, Hicklin DJ, Ellis LM. Antiangiogenic therapy--evolving view based on clinical trial results. Nature reviews Clinical oncology. 2012; 9:297–303.
41. Marshall MV, Draney D, Sevick-Muraca EM, Olive DM. Single-dose intravenous toxicity study of IRDye 800CW in Sprague-Dawley rats. Molecular imaging and biology: MIB: the official publication of the Academy of Molecular Imaging. 2010; 12:583–594. [PubMed: 20376568]
42. Biosciences, L-C. IRDye(R) 800CW Protein Labeling Kit - High MW. Lincoln, Nebraska: LI-COR Biosciences; 2007. p. 1-9.
43. Day KE, Sweeny L, Kulbersh B, Zinn KR, Rosenthal EL. Preclinical comparison of near-infrared-labeled cetuximab and panitumumab for optical imaging of head and neck squamous cell carcinoma. Mol Imaging Biol. 2013; 15:722–729. [PubMed: 23715932]
44. Atkins D, Reiffen KA, Tegtmeier CL, Winther H, Bonato MS, Storkel S. Immunohistochemical detection of EGFR in paraffin-embedded tumor tissues: variation in staining intensity due to

choice of fixative and storage time of tissue sections. The journal of histochemistry and cytochemistry: official journal of the Histochemistry Society. 2004; 52:893–901. [PubMed: 15208356]

45. Sweeny L, Dean NR, Magnuson JS, et al. EGFR expression in advanced head and neck cutaneous squamous cell carcinoma. Head & neck. 2012; 34:681–686. [PubMed: 21739514]
46. Chung TK, Warram J, Day KE, Hartman Y, Rosenthal EL. Time-dependent pretreatment with bevacuzimab increases tumor specific uptake of cetuximab in preclinical oral cavity cancer studies. Cancer Biol Ther. 2015; 16:790–798. [PubMed: 25719497]
47. Reuthebuch O, Haussler A, Genoni M, et al. Novadaq SPY: intraoperative quality assessment in off-pump coronary artery bypass grafting. Chest. 2004; 125:418–424. [PubMed: 14769718]
48. Liu D, Liu X, Xing M. Activities of multiple cancer-related pathways are associated with BRAF mutation and predict the resistance to BRAF/MEK inhibitors in melanoma cells. Cell Cycle. 2014; 13:208–219. [PubMed: 24200969]
49. Gross A, Niemetz-Rahn A, Nonnenmacher A, Tucholski J, Keilholz U, Fusi A. Expression and activity of EGFR in human cutaneous melanoma cell lines and influence of vemurafenib on the EGFR pathway. Targeted oncology. 2015; 10:77–84. [PubMed: 24824730]
50. Heath CH, Deep NL, Sweeny L, Zinn KR, Rosenthal EL. Use of panitumumab-IRDye800 to image microscopic head and neck cancer in an orthotopic surgical model. Ann Surg Oncol. 2012; 19:3879–3887. [PubMed: 22669455]
51. Kulbersh BD, Duncan RD, Magnuson JS, Skipper JB, Zinn K, Rosenthal EL. Sensitivity and specificity of fluorescent immunoguided neoplasm detection in head and neck cancer xenografts. Archives of otolaryngology--head & neck surgery. 2007; 133:511–515. [PubMed: 17520766]
52. Rosenthal EL, Kulbersh BD, Duncan RD, et al. In vivo detection of head and neck cancer orthotopic xenografts by immunofluorescence. Laryngoscope. 2006; 116:1636–1641. [PubMed: 16954995]
53. Willett CG, Boucher Y, di Tomaso E, et al. Direct evidence that the VEGF-specific antibody bevacizumab has antivascular effects in human rectal cancer. Nature medicine. 2004; 10:145–147.
54. Willett CG, Boucher Y, Duda DG, et al. Surrogate markers for antiangiogenic therapy and dose-limiting toxicities for bevacizumab with radiation and chemotherapy: continued experience of a phase I trial in rectal cancer patients. Journal of clinical oncology: official journal of the American Society of Clinical Oncology. 2005; 23:8136–8139. [PubMed: 16258121]
55. Willett CG, Duda DG, di Tomaso E, et al. Efficacy, safety, and biomarkers of neoadjuvant bevacizumab, radiation therapy, and fluorouracil in rectal cancer: a multidisciplinary phase II study. Journal of clinical oncology: official journal of the American Society of Clinical Oncology. 2009; 27:3020–3026. [PubMed: 19470921]
56. Yamanaka K, Nakahara T, Yamauchi T, et al. Antitumor activity of YM155, a selective small-molecule survivin suppressant, alone and in combination with docetaxel in human malignant melanoma models. Clin Cancer Res. 2011; 17:5423–5431. [PubMed: 21737502]
57. Liu Q, Mier JW, Panka DJ. Differential modulatory effects of GSK-3beta and HDM2 on sorafenib-induced AIF nuclear translocation (programmed necrosis) in melanoma. Mol Cancer. 2011; 10:115. [PubMed: 21929745]
58. Arjaans M, Oosting SF, Schroder CP, de Vries EG. Bevacizumab-induced vessel normalization hampers tumor uptake of antibodies--response. Cancer research. 2013; 73:7147–7148. [PubMed: 24265275]
59. Hadjipanayis CG, Jiang H, Roberts DW, Yang L. Current and future clinical applications for optical imaging of cancer: from intraoperative surgical guidance to cancer screening. Seminars in oncology. 2011; 38:109–118. [PubMed: 21362519]
60. Keereweer S, Kerrebijn JD, Mol IM, et al. Optical imaging of oral squamous cell carcinoma and cervical lymph node metastasis. Head & neck. 2012; 34:1002–1008. [PubMed: 21987435]

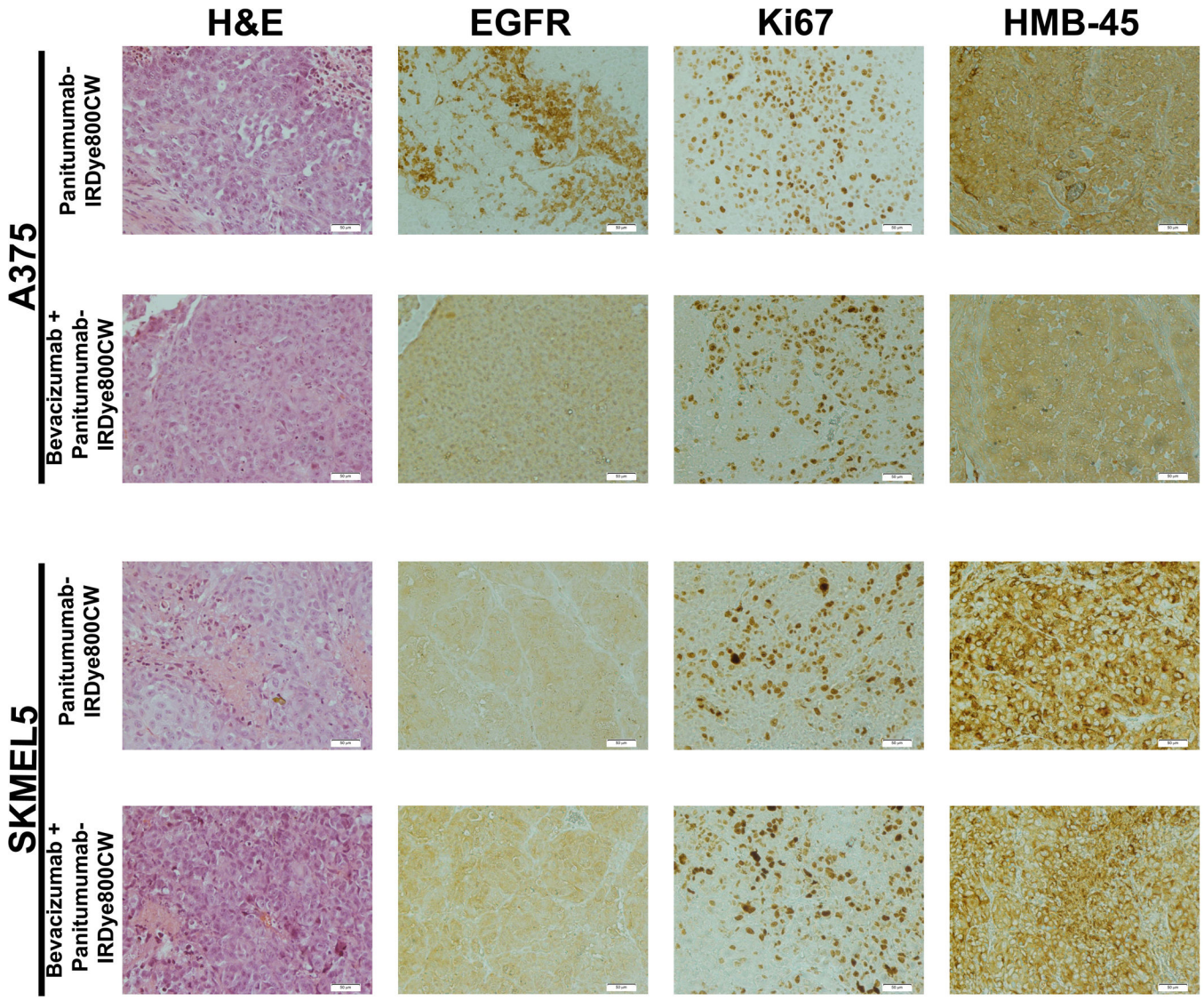

Figure 1.

Histologic assessment of A375 and SKMEL5 tumor specimens 14 days after systemic injection of panitumumab-IRDye800CW or pretreatment with bevacizumab followed by panitumumab-IRDye800CW. Initial staining was with hematoxylin and eosin (H&E). Epidermal growth factor receptor (EGFR) immunohistochemical staining and reactivity analysis was performed. Membrane EGFR reactivity was based on the following scores: 0 = no staining to < 10% of tumor cells staining, 1+ = light and incomplete staining in > 10% of tumor cells, 2+ = moderate and complete staining of > 10% of tumor cells and 3+ = intense and complete staining > 10%. Ki67 staining was done to evaluate to cell viability after therapy. Human melanoma black (HMB-45) anti-melanoma antibody was performed to confirm melanoma tumor cells.

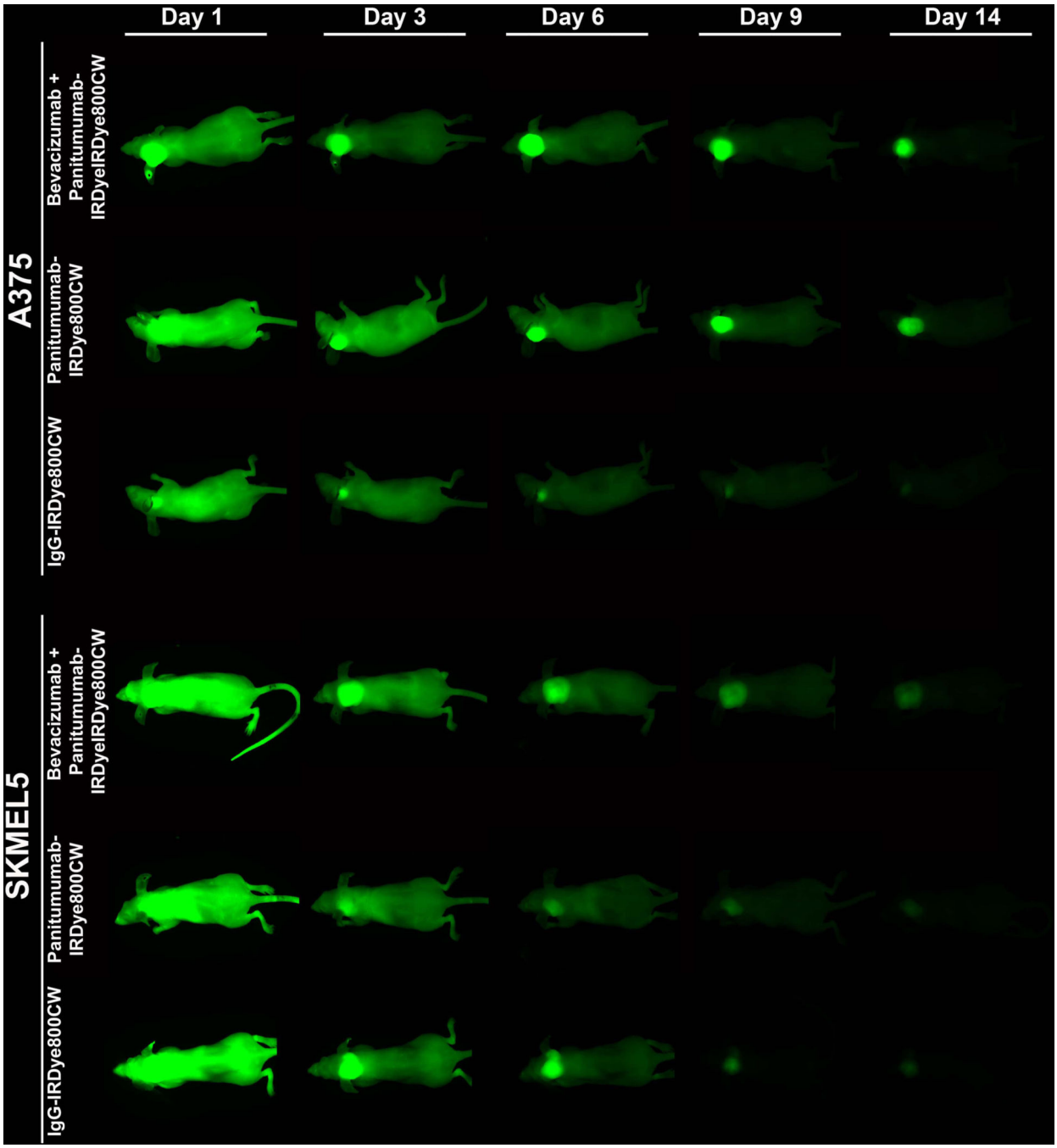

Figure 2.

Imaging of mice with ear melanoma xenografts (A375 or SKMEL5) was done with the Pearl device (closed system with a cooled charge-coupled camera). Imaging was done daily (select days shown) following systemic injection of either panitumumab-IRDye800CW or IgG-IRDye800CW (200ug, tail vein). To examine the effect of pretreatment with bevacizumab on panitumumab delivery, the bevacizumab (5 mg/kg) was injected 3 days prior to administration of panitumumab-IRDye800CW.

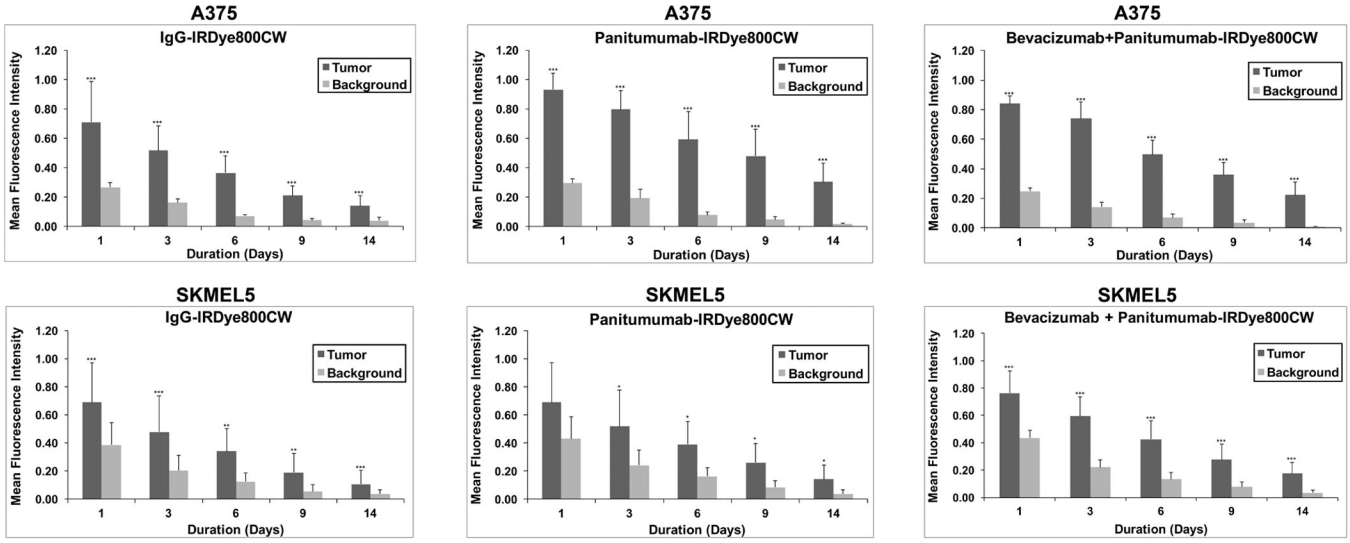

Figure 3.

Graphical representation of fluorescence within the mouse ear melanoma xenografts (A375 and SKMEL5) on days 3, 6, 9, and 12 via imaging with the Pearl device. Column, mean for treatment group (n=5); bars, standard deviation. Statistical significance by unpaired t-test, *p<0.05, **p<0.01, ***p<0.001.

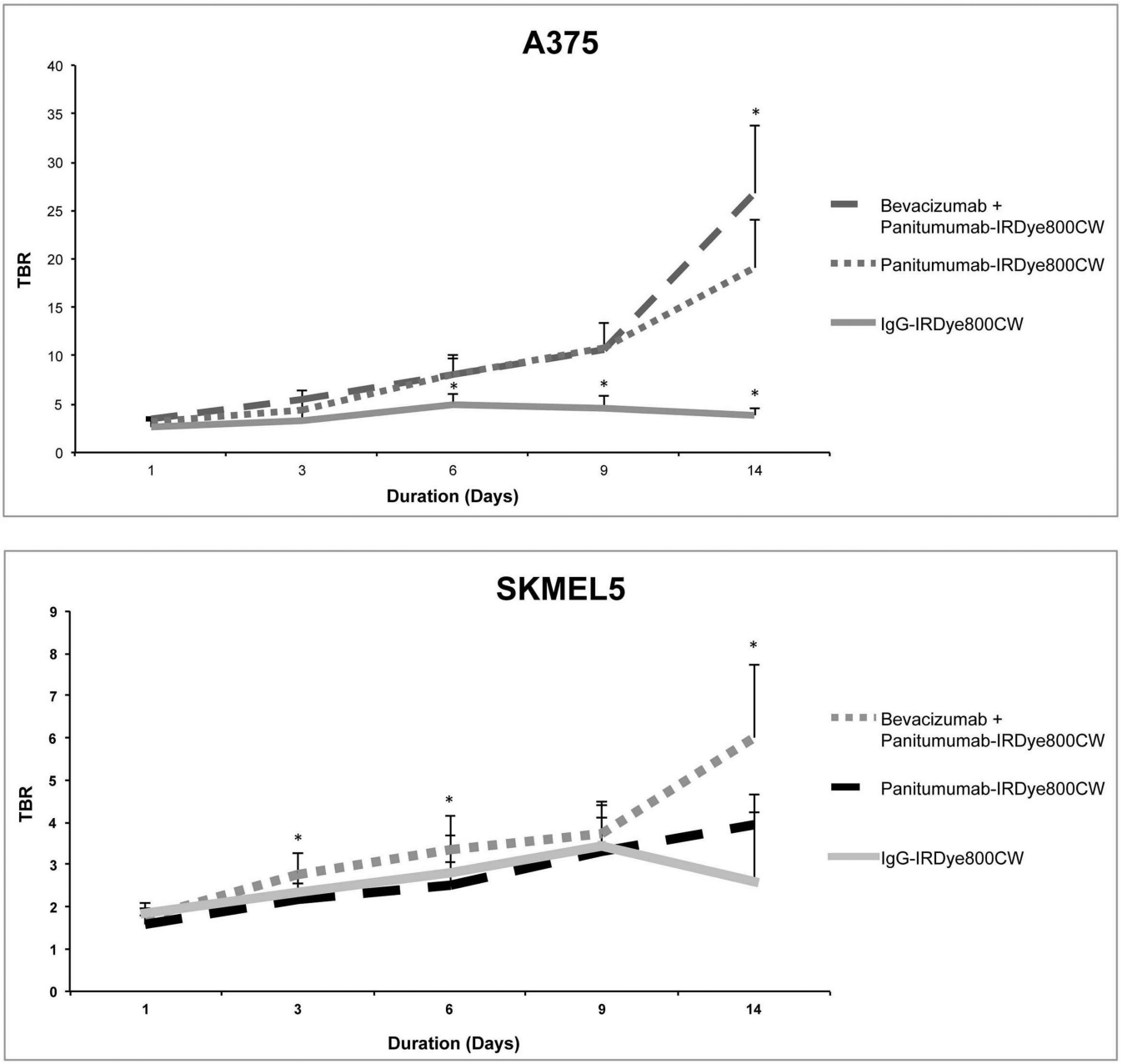

Figure 4.

The fluorescence for the tumor-to-background ratio (TBR) was calculated using images obtained on the Pearl device of mouse ear xenografts (A4375 and SMEL5). Bars, standard deviation. Statistical significance by unpaired t-test, *p<0.05.

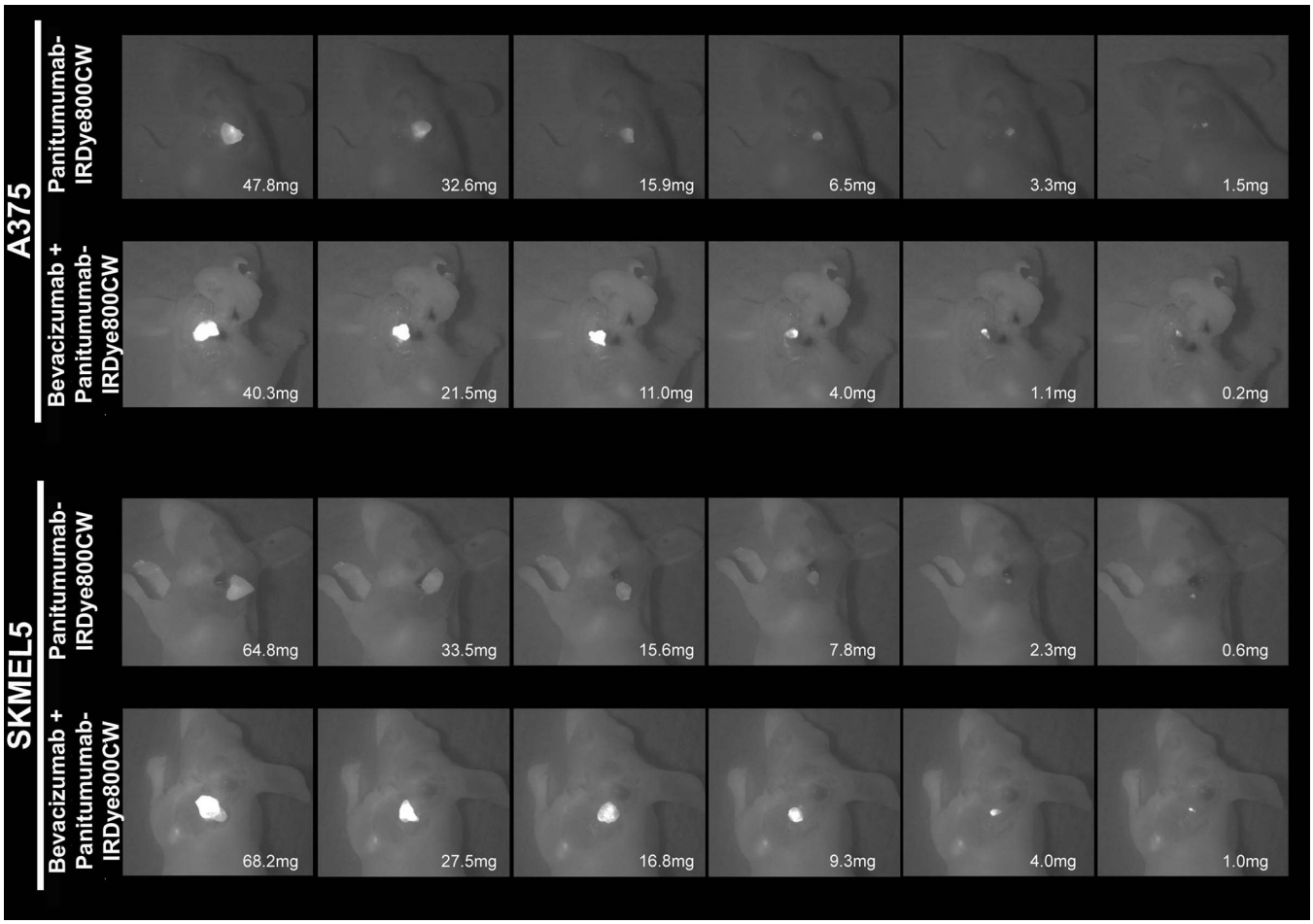

Figure 5.

Fluorescence guided surgical resection was done on day 14 at the time of tumor harvest. The LUNA was used to provide real-time imaging during the resection. Serial sections were taken to determine the lowest mass detectable for each group.

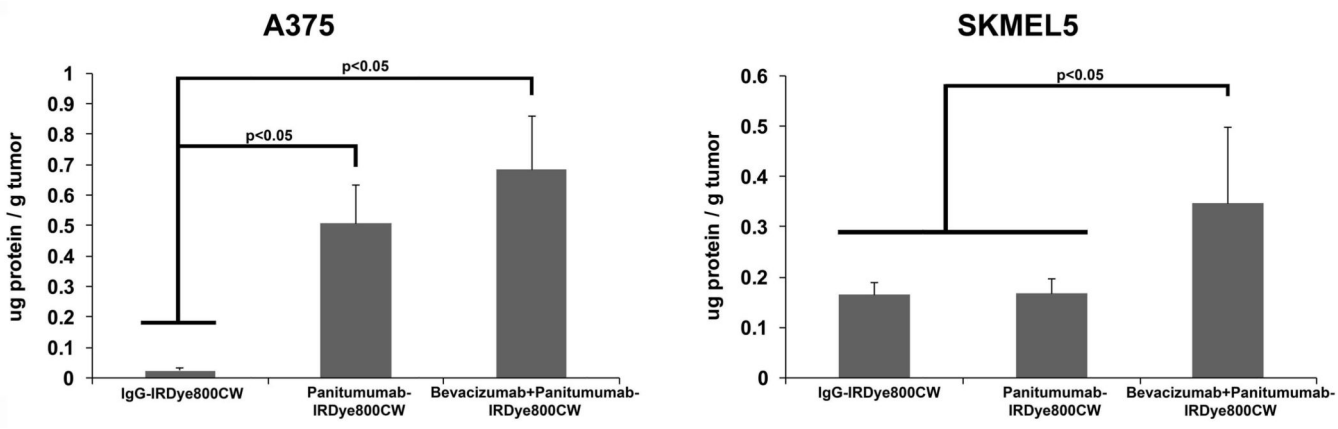

Figure 6.

Normalized standards with known concentrations of panitumumab-IRDye800CW or IgG-IRDye800CW were used to calculate drug uptake by the melanoma tumors (A375 and SKMEL5).